Contributions to Mineralogy and Petrology (2018) 173:52
https://doi.org/10.1007/s00410-018-1478-x

ORIGINAL PAPER

Transition metals in the transition zone: partitioning of Ni, Co, and Zn between olivine, wadsleyite, ringwoodite, and clinoenstatite

Li Zhang[1,2] · Joseph R. Smyth[2] · Takaaki Kawazoe[3,4] · Steven D. Jacobsen[5] · Shan Qin[1]

Received: 6 February 2018 / Accepted: 31 May 2018 / Published online: 8 June 2018

Abstract

Ni, Co, and Zn are widely distributed in the Earth's mantle as significant minor elements that may offer insights into the chemistry of melting in the mantle. To better understand the distribution of Ni^{2+}, Co^{2+}, and Zn^{2+} in the most abundant silicate phases in the transition zone and the upper mantle, we have analyzed the crystal chemistry of wadsleyite (Mg_2SiO_4), ringwoodite (Mg_2SiO_4), forsterite (Mg_2SiO_4), and clinoenstatite ($Mg_2Si_2O_6$) synthesized at 12–20 GPa and 1200–1400 °C with 1.5–3 wt% of either NiO, CoO, or ZnO in starting materials. Single-crystal X-ray diffraction analyses demonstrate that significant amounts of Ni, Co, and Zn are incorporated in octahedral sites in wadsleyite (up to 7.1 at%), ringwoodite (up to 11.3 at%), olivine (up to 2.0 at%), and clinoenstatite (up to 3.2 at%). Crystal structure refinements indicate that crystal field stabilization energy (CFSE) controls both cation ordering and transition metal partitioning in coexisting minerals. According to electron microprobe analyses, Ni and Co partition preferentially into forsterite and wadsleyite relative to coexisting clinoenstatite. Ni strongly prefers ringwoodite over coexisting wadsleyite with $D_{Ni}^{Rw/Wd} = 4.13$. Due to decreasing metal–oxygen distances with rising pressure, crystal field effect on distribution of divalent metal ions in magnesium silicates is more critical in the transition zone relative to the upper mantle. Analyses of Ni partitioning between the major upper-mantle phases implies that Ni-rich olivine in ultramafic rocks can be indicative of near-primary magmas.

Keywords Transition zone · X-ray diffraction · Cation ordering · Element distribution

Introduction

Forsterite (Mg_2SiO_4) is the magnesium end-member of olivine $(Mg, Fe)_2SiO_4$, the major mineral phase in the Earth's upper mantle (e.g., Harris et al. 1967). The crystal structure of forsterite (space group *Pbnm*) has two symmetrically distinct octahedral sites (M1 and M2), one tetrahedral site, and three distinct oxygen positions (O1, O2, and O3). In forsterite, tetrahedral Si is isolated, but connected by a network of edge-sharing octahedral Mg sites (e.g., Birle et al. 1968). At a depth of about 410 km, forsterite transforms to wadsleyite (Mg_2SiO_4), which corresponds to the spinelloid III structure. Wadsleyite (space group *Imma*) is a sorosilicate, containing three symmetrically distinct divalent octahedral sites: M1, M2, and M3, one tetrahedral site, and four distinct oxygen positions: O1, O2, O3, and O4. The pairs of linked tetrahedral sites form Si_2O_7 dimers (e.g., Akaogi et al. 1982). At a depth of about 520 km, wadsleyite transforms to ringwoodite, which has the spinel structure (space group $Fd\bar{3}m$). Ringwoodite contains one tetrahedral Si site and one highly symmetric octahedral (M) site (point symmetry $\bar{3}m$),

The original version of this article was revised with Table 1.

Communicated by Timothy L. Grove.

Electronic supplementary material The online version of this article (https://doi.org/10.1007/s00410-018-1478-x) contains supplementary material, which is available to authorized users.

✉ Li Zhang
li.z.zhang@colorado.edu

[1] School of Earth and Space Sciences, Peking University, Beijing 100871, China

[2] Department of Geological Sciences, University of Colorado, Boulder, CO 80309, USA

[3] Bayerisches Geoinstitut, University of Bayreuth, 95440 Bayreuth, Germany

[4] Department of Earth and Planetary Systems Science, Hiroshima University, Higashi-Hiroshima 739-8526, Japan

[5] Department of Earth and Planetary Sciences, Northwestern University, Evanston, IL 60208, USA

in which the distances of six metal–oxygen bonds are all equivalent (e.g., Ringwood 1958).

As the magnesium end-member of pyroxene, enstatite ($MgSiO_3$) has been studied experimentally in previous studies. In the enstatite structure, divalent cations occupy two octahedral sites (M1 and M2) which are linked by chains of SiO_4 tetrahedra. The M1 site is slightly distorted from octahedral symmetry. The M2 site, by contrast, has larger octahedral volume and it is very distorted (e.g., Morimoto et al. 1960; Ringwood 1967). The stable phase of $MgSiO_3$ at ambient pressure and temperature is low clinoenstatite (with space group $P2_1/c$, containing two distinct tetrahedral sites: Si1 and Si2, and six distinct oxygen positions: O1, O2, O3, O4, O5, and O6), with orthoenstatite (space group *Pbca*), containing two distinct tetrahedral sites: Si1 and Si2, and six distinct oxygen positions O1, O2, O3, O4, O5, and O6 becoming stable above 600 °C. At pressures over 7 GPa, structure transformation from low-clinoenstatite to high-clinoenstatite (space group $C2/c$) containing one tetrahedral site, and three distinct oxygen positions: O1, O2, and O3 is observed (e.g., Angel et al. 1992). For high-pressure sample synthesis, the high-clinoenstatite ($C2/c$) phase always reverts displacively to $P2_1/c$ on quench (e.g., Smyth 1969). Nestola et al. (2004) analyzed clinopyroxene of composition $Ca_{0.15}Mg_{1.85}Si_2O_6$ ($Di_{15}En_{85}$) at pressure up to 6.5 GPa and detected $P2_1/c-C2/c$ displacive phase transition at 5.1 GPa. In addition, they demonstrated that clinopyroxene ($Ca_{0.15}Mg_{1.85}Si_2O_6$) with $C2/c$ space group can occur at room pressure and about 1370 °C. The transformation from low to high-clinoenstatite is characterized by the differences in the configuration of their silicate chains. In the structure of low clinoenstatite, there are two symmetrically distinct tetrahedral chains rotated in opposite directions, whereas in high-clinoenstatite, there is only one symmetrically distinct tetrahedral chain (Angel et al. 1992).

According to previous chemical analyses of mantle xenoliths, ophiolite sequences and basalt petrogenesis (Anderson 1983; Liu and Bassett 1986; McDonough and Sun 1995; Hofmann 1988), the concentrations of Ni and Co are estimated to be 2080 and 104 ppm in the Earth's primitive mantle, and those of Ni, Co, and Zn are estimated to be 1960, 105, and 55 ppm in the pyrolite model. As inclusions in diamonds, olivines with high NiO contents (up to 0.64 wt%) in the deep upper mantle (Stachel and Harris 2008) and Fe–Ni alloy in the lower mantle have been observed (Smith et al. 2016). Hacker et al. (1997) reported high-Ni olivines (0.4 wt% NiO) in peridotites from the Alpe Arami massif which were interpreted as a piece of the mantle transition zone (e.g., Dobrzhinetskaya et al. 1996; Green et al. 1997). Chemical analyses of natural olivine show that Ni^{2+}, Co^{2+}, and Zn^{2+} are common constituents (e.g., de Waal 1978), and the distribution of these divalent minor metal cations at different crystallographic sites in olivine have been previously studied (e.g., Hakli and Wright 1967; Annersten et al. 1982). Paramagnetically shifted NMR resonances indicate that, in forsterite, Ni^{2+} occupies only M1, Fe^{2+} occupies M1 and M2 roughly equally, and Co^{2+} occupies both M1 and M2 in an approximately 3:1 ratio (McCarty et al. 2015).

Finger et al. (1993) refined the crystal structures of synthetic wadsleyite $(Mg, Fe)_2SiO_4$, revealing that Fe^{2+} is depleted in the M2 octahedron, whereas it is enriched in M1 and M3. The same strong ordering of Fe was observed by Smyth et al. (2014) in relatively hydrous and oxidized wadsleyite. Zhang et al. (2016) synthesized wadsleyites coexisting with clinoenstatites with 3 wt% of either CoO, NiO, or ZnO under hydrous conditions in separate experiments at 1300 °C and 15 GPa. The refined crystal structures of these wadsleyites display site preferences of Ni^{2+}, Co^{2+}, and Zn^{2+} similar to those of Fe^{2+} with $M1 \approx M3 > M2$.

The ordering of divalent cations in orthopyroxene has been determined by previous experimental studies (e.g., Bancroft and Burns 1967; Ghose et al. 1975), whereas those in high-pressure clinoenstatite are comparatively unconstrained. For orthopyroxene, according to Ghose et al. (1975), Co^{2+} and Zn^{2+} are both relatively enriched in M2, while Ni^{2+} are enriched in M1.

The distribution of divalent metal cations between coexisting ferromagnesian silicates in the mantle has been widely investigated. According to previous observations, Ni^{2+} and Co^{2+} are enriched in olivine relative to orthopyroxene (e.g., Hakli and Wright 1967; Mercy and O'Hara 1967). Gudfinnsson and Wood (1998) conducted multi-anvil experiments at 1400–1600 °C on olivine and peridotite starting compositions (Fo_{85}–Fo_{90}) to determine the partitioning of Ni^{2+} and Ca^{2+} between coexisting olivine and wadsleyite, demonstrating that Ni^{2+} partitions preferentially into wadsleyite relative to olivine, whereas Ca^{2+} tends to be enriched in olivine compared to wadsleyite. Zhang et al. (2016) demonstrated that significant amounts of NiO, CoO, and ZnO can be incorporated in wadsleyite (3–6 wt%), suggesting that the solubility of these minor oxides in wadsleyite is higher than those in the coexisting clinoenstatite and upper-mantle olivine.

To better constrain the distribution of divalent metal ions between coexisting minerals in the transition zone and the overlying upper mantle, the crystal structures of coexisting wadsleyite (Mg_2SiO_4) and ringwoodite (Mg_2SiO_4) synthesized with minor NiO in starting materials, coexisting wadsleyite (Mg_2SiO_4) and clinoenstatite ($Mg_2Si_2O_6$) and coexisting olivine (Mg_2SiO_4) and clinoenstatite synthesized with minor NiO, CoO, or ZnO were studied by electron microprobe and single crystal X-ray diffraction methods. The principal factors that control cation ordering and distribution in coexisting minerals in the upper mantle and the transition zone are discussed based on analysis of their crystal chemistry.

Experimental work

Synthesis

Samples were synthesized in a 1200 tonne Sumitomo multi-anvil press at Bayerisches Geoinstitut, University of Bayreuth, Germany. Coexisting wadsleyite and ringwoodite (SS1504) were synthesized at 20 GPa and quenched from 1400 °C, using 10/5 assemblies (10 mm MgO octahedron with 5 mm corner truncations). Coexisting olivine and clinoenstatite (SS1604A-C) were synthesized at 12 GPa and quenched from 1200 °C, using 14/8 assemblies. Starting materials were mixed from oxides of SiO_2 (quartz), MgO (periclase), $Mg(OH)_2$ (brucite) plus 1.5 wt% of either NiO, ZnO or CoO, in separate capsules for coexisting olivine and clinoenstatite, and plus 3 wt% NiO and 1.0 wt% water (H_2O) as brucite in the starting material for coexisting wadsleyite and ringwoodite, i.e., the solubility of water in wadsleyite at 1400 °C measured in the Mg_2SiO_4 system (Demouchy et al. 2005). Heating duration was the same across all runs at 220 min. Quench to temperatures below 500 °C took about 3 s. Recovered capsules were mounted in epoxy on 24 mm round glass slides and ground to expose the run products. The experimental details of sample synthesis for coexisting SS1405-1407 wadsleyite and clinoenstatite (synthesized at 15 GPa, 1300 °C) were previously reported by Zhang et al. (2016). The experimental conditions of sample synthesis and phase compositions are summarized in Table 1. BSE images of coexisting minerals for SS1504 wadsleyite and ringwoodite, SS1406 wadsleyite and clinoenstatite, and SS1604 A-C olivine and clinoenstatite are shown in Fig. 1.

Electron microprobe analysis

Mineral compositions were analyzed using a JEOL 8900 electron microprobe (EPMA) at the Institute of Geology, Chinese Academy of Geological Sciences. Acceleration voltage was 15 kV, beam current was 20 nA, and beam size was 5–1 μm. Standards for Mg and Si were Fo_{90} olivine, Ni—nickel metal, Co—cobalt metal, Zn—sphalerite. The results of electron microprobe analysis were listed in Appendix Table 1. Mineral compositions of SS1405-1407 wadsleyite and SS1405,1407 clinoenstatite were previously reported by Zhang et al. (2016).

X-ray diffraction

Single-crystal samples (SS1504 wadsleyite and ringwoodite; SS1405-1407 clinoenstatite; SS1604A-C olivine and clinoenstatite) were chosen from the capsules and mounted on glass fibers and centered on a four-circle diffractometer for X-ray diffraction analysis. Intensity data were collected with a Bruker APEX II CCD detector on a Siemens/MAC-Science 18 kW rotating Mo-anode X-ray generator at the University of Colorado, Boulder. 50 kV voltage, 250 mA current and calibrated radiation ($\lambda = 0.71073$ Å) were used for all measurements. Crystal structures, atom positions, occupancies, and displacement parameters were refined from the intensity data sets using SHELXL-97 in the package WINGX (e.g., Sheldrick 1997). To match the refinement model used in Zhang et al. (2016), scattering factors for ionized cations Mg^{2+}, Si^{4+}, Co^{2+}, Ni^{2+}, Zn^{2+} (Cromer and Mann 1968), and O^{2-} (Tokonami 1965) were used, as these were found to give both accurate structural geometry and reliable site occupancy (within 1 at%) refinements for pure Mg phases (Smyth et al. 2004, 2014; Ye et al. 2009; Zhang et al. 2016). For site occupancies, electron-in-bond model (Heinemann model) is considered to give more precise (better than 1 at%) determination compared to the refinement strategy in this study (Angel and Nestola 2016). Lattice parameters and data collection parameters are listed in Appendix Table 2, atom positions are given in Appendix Tables 3, 4, and 5, site geometries and occupancy factors are shown in Appendix Tables 6, 7, and 8. The X-ray diffraction analyses for wadsleyite (SS1405-1407) were previously reported by Zhang et al. (2016).

Table 1 Experimental conditions of sample synthesis and phase composition

Experiment No.	Starting composition	Pressure (GPa)	Temperature (°C)	Duration (h)	Phase composition
SS1504	Mg_2SiO_4 + 3 wt% NiO + 1 wt% H_2O	20	1400	3.6	Wadsleyite + ringwoodite
SS1604A	$Mg_{1.84}Si_{1.08}O_4$ + 1.5 wt% NiO + 0.5 wt% H_2O	12	1200	3.6	Olivine + clinoenstatite
SS1604B	$Mg_{1.84}Si_{1.08}O_4$ + 1.5 wt% CoO + 0.5 wt% H_2O	12	1200	3.6	Olivine + clinoenstatite
SS1604C	$Mg_{1.84}Si_{1.08}O_4$ + 1.5 wt% ZnO + 0.5 wt% H_2O	12	1200	3.6	Olivine + clinoenstatite
SS1405	$Mg_{1.84}Si_{1.08}O_4$ + 3 wt% CoO + 1 wt% H_2O	15	1300	3.6	Wadsleyite + clinoenstatite
SS1406	$Mg_{1.84}Si_{1.08}O_4$ + 3 wt% NiO + 1 wt% H_2O	15	1300	3.6	Wadsleyite + clinoenstatite
SS1407	$Mg_{1.84}Si_{1.08}O_4$ + 3 wt% ZnO + 1 wt% H_2O	15	1300	3.6	Wadsleyite + clinoenstatite

Sample SS1405-1406 were previously synthesized by Zhang et al. (2016)

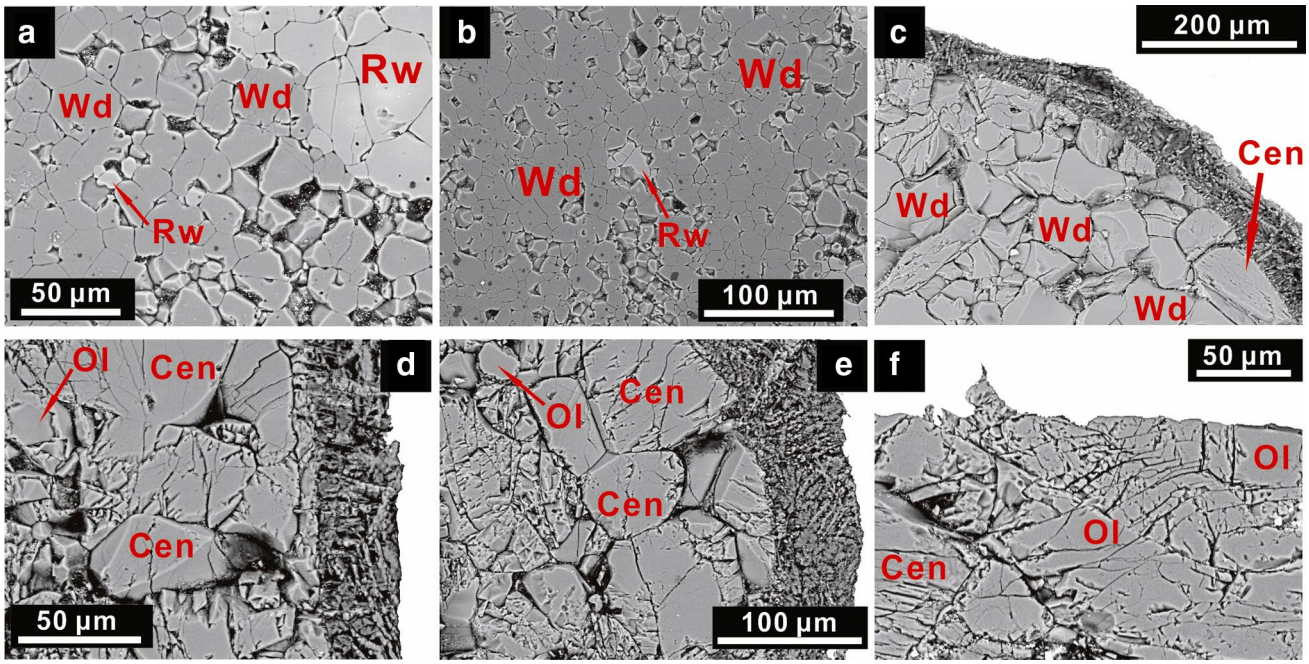

Fig. 1 Backscattered electron (BSE) images of coexisting minerals. **a, b** SS1504 wadsleyite and ringwoodite. **c** SS1406 wadsleyite and clinoenstatite. **d–f** SS1604A-C olivine and clinoenstatite. *Wd* wadsleyite, *Rw* ringwoodite, *Ol* olivine, and *Cen* clinoenstatite. BSE images of SS1405, 1407 wadsleyite and clinoenstatite are shown in Zhang et al. (2016)

Results

As shown in Table 2, the results of single-crystal X-ray diffraction demonstrate that significant amounts of Ni, Co, and Zn are incorporated in octahedral sites in wadsleyite (up to 7.1 at%), ringwoodite (up to 11.3 at%), olivine (up to 2.0 at%), and clinoenstatite (up to 3.2 at%). Ni^{2+}, Co^{2+}, and Zn^{2+} substitute into both M1 and M2 sites in olivine (SS1604A-C) and clinoenstatite (SS1604A-C; SS1405-1407). For olivine, Ni and Co prefer M1, whereas Zn shows a slight preference for M2. Octahedral site occupancy ratios (M2/M1) were estimated to be 0.5 for Ni^{2+}, 0.35 for Co^{2+}, and 1.5 for Zn^{2+} (Table 3) based on the occupancy factors listed in Table 2. For coexisting clinoenstatite (SS1604A-C), Ni^{2+} is more compatible in M1 site, whereas both Co^{2+} and Zn^{2+} avoid M1 relative to M2 (Table 2), and the site occupancy ratios (M2/M1) were calculated to be 0.67 for Ni^{2+}, 1.42 for Co^{2+}, and 1.14 for Zn^{2+} (Table 3). In contrast, clinoenstatite (SS1405-1407) coexisting with wadsleyite displays different site preferences; Co^{2+} prefers M1 over M2 (Table 2), and the site occupancy ratios (M2/M1) were estimated to be 0.25 for Ni^{2+}, 0.5 for Co^{2+}, and 1.07 for Zn^{2+} (Table 3). For wadsleyite (SS1504), Ni^{2+} displays strong site preferences similar to previous observed cation orderings of Ni^{2+}, Co^{2+}, and Zn^{2+} (SS1405-1407; Zhang et al. 2016) with $M1 \approx M3 > M2$.

Partition coefficients of Ni, Co, and Zn in coexisting minerals (Table 3) were calculated on the basis of electron microprobe analysis (Table 3; Appendix Table 1), suggesting that Ni and Co are preferentially incorporated into olivine relative to clinoenstatite (SS1604A-C) with $D_{Ni}^{Ol/Cen} = 2.46$; $D_{Co}^{Ol/Cen} = 2.07$, while Zn shows only a slight preference for partitioning between olivine and clinoenstatite with $D_{Zn}^{Ol/Cen} = 1.19$. For coexisting wadsleyite and clinoenstatite (SS1405-1407), Ni, Co, and Zn preferentially partition into wadsleyite in the same order $D_{Ni}^{Wd/Cen} > D_{Co}^{Wd/Cen} > D_{Zn}^{Wd/Cen}$ with $D_{Ni}^{Wd/Cen} = 4.18$; $D_{Co}^{Wd/Cen} = 3.54$; $D_{Zn}^{Wd/Cen} = 2.43$. Consistent with electron microprobe analysis, as shown in Table 3, partition coefficients ($D^{Wd/Cen}$ and $D^{Ol/Cen}$) estimated based on single-crystal X-ray diffraction also decrease in the order Ni > Co > Zn. For coexisting wadsleyite and ringwoodite (SS1504), partition coefficient of Ni^{2+} ($D_{Ni}^{Rw/Wd}$) was estimated to be 4.13, indicating that ringwoodite has higher capability of incorporating Ni^{2+} relative to wadsleyite.

Discussion

Cation ordering of Ni, Co, and Zn in the mantle phases

Cation ordering in a crystal structure can be influenced by cation size, crystal field stabilization energy, and site distortion (e.g., Ghose et al. 1975; Burns 1993). Consistent with previous studies (e.g., Birle et al. 1968), in olivine we observe a tetragonally distorted M1 site, elongated in the

Table 2 Occupancy parameters (at%) of divalent cations

		Wadsleyite*			
		M1	M2	M3	Si
SS1406 Ni^{2+}		7.1 (5)	2.6 (5)	4.5 (4)	1.1 (5)
SS1405 Co^{2+}		4.3 (3)	2.7 (3)	4.2 (3)	2.4 (4)
SS1407 Zn^{2+}		2.7 (4)	2.0 (4)	2.9 (0)	0.6 (3)
SS1504 Ni^{2+}		2.2 (1)	0.8 (1)	1.8 (2)	0.0
	Ringwoodite				
	M				Si
SS1504 Ni^{2+}	11.3(6)				0.0
		Olivine			
		M1	M2	Si	
SS1604A Ni^{2+}		2.0(2)	1.0(3)	0.0	
SS1604B Co^{2+}		1.7(3)	0.6(3)	0.0	
SS1604C Zn^{2+}		0.6(3)	0.9(3)	0.0	
		Clinoenstatite			
		M1	M2	Si1	Si2
SS1406 Ni^{2+}		3.2 (3)	0.8 (3)	0.0	0.0
SS1405 Co^{2+}		2.8 (3)	1.4 (3)	0.0	0.0
SS1407 Zn^{2+}		2.8 (3)	3.0 (3)	0.0	0.0
SS1604A Ni^{2+}		2.1 (3)	1.4 (3)	0.0	0.0
SS1604B Co^{2+}		1.2 (3)	1.7 (3)	0.0	0.0
SS1604C Zn^{2+}		1.4 (3)	1.6 (2)	0.0	0.0

*Site occupancy parameters for SS1405-1407 wadsleyites were previously reported by Zhang et al. (2016)

direction of the two M1–O3 bonds, whereas M2 is trigonally distorted and has larger polyhedral volume compared to M1 (Fig. 2; Appendix Tables 7). Considering that the high-spin octahedral ionic radii of Ni^{2+}, Mg^{2+}, Zn^{2+}, and Co^{2+} increase in the order Ni^{2+} (69 pm) < Mg^{2+} (72 pm) < Zn^{2+} (74 pm) < Co^{2+} (74.5 pm) (Shannon 1976; Huheey 1983), Ni^{2+} is expected to be enriched in M1 relative to larger M2, while Co^{2+} and Zn^{2+} are expected to preferentially occupy M2. However, consistent with previous observations on cation ordering in olivine (e.g., Annersten et al. 1982; McCarty et al. 2015), the M site occupancy values (Table 2) show that Co^{2+} prefers smaller M1 over larger M2, indicating that cation size is not the primary factor affecting the site preferences in olivine.

According to crystal field theory, for high-spin configurations, Ni^{2+} has 6 electrons in t_{2g} orbitals and 2 electrons in e_g orbitals, leading to a larger crystal field stabilization energy (CFSE) than Co^{2+}, which has 5 t_{2g} electrons and 2 e_g electrons in the crystal field splitting of the octahedral site. Since the $3d$ orbitals of Zn^{2+} are fully occupied by 10 electrons, Zn^{2+} has no CFSE in octahedra (Burns 1993). For divalent cations, the CFSE in regular octahedra are estimated in the order Ni^{2+} (−29 kcal/mol) < Co^{2+} (−21 kcal/mol) < Zn^{2+} (zero) = Mg^{2+} (zero) (Dunitz and Orgel 1957; McClure 1957). Considering that the values of CFSE are higher for smaller sites (Burns 1993), both Ni^{2+} and Co^{2+} are expected to be enriched in M1 relative to M2. In addition, for olivine M1, the tetragonal distortion of this octahedron which is elongated along tetrad axis (Fig. 2) increases the stability of the ions with $3d^7$ high-spin configuration (Burns 1993). As a result, Co^{2+} is expected to display a stronger preference for olivine M1, although Co^{2+} has a lower CFSE value than Ni^{2+} in regular octahedra. As shown in Fig. 3, the observed cation ordering of Ni^{2+}, Co^{2+}, and Zn^{2+} for refined olivine crystals (SS1604A-C) can be explained by crystal field theory, indicating that CFSE is the key factor affecting the site enrichments of those minor transition metal ions in olivine.

For all clinoenstatite samples, consistent with previous studies (e.g., Morimoto et al. 1960; Ringwood 1967), M2 is larger and more distorted than M1. In the M2 octahedron, the quadrilateral consisting of O1, O3, O4, and O6 with four unequal M–O bonds is highly asymmetrical (Fig. 2; Appendix Table 8). As shown in Fig. 3, for clinoenstatites synthesized at 12 GPa (SS1604A-C), the estimated occupancy ratios (M2/M1) of Ni^{2+}, Co^{2+}, and Zn^{2+} display a

Table 3 Octahedral site occupançy raitos, minor metal oxide content, and estimated partition coefficient of divalent cations for coexisting minerals

	M site Occ raito[a]		Minor metal oxide content (wt%)[b]		Partition coefficient (EMPA)[c]	Partition coefficient (XRD)[d]
	Wadsleyite (M2/(M1 + M3))	Clinoenstatite (M2/M1)	Wadsleyite	Clinoenstatite	$D^{Wadsleyite/Clinoenstatite}$	$D^{Wadsleyite/Clinoenstatite}$
SS1406 Ni	0.22	0.25	5.98	1.43	4.18	3.65
SS1405 Co	0.32	0.50	3.40	0.96	3.54	3.43
SS1407 Zn	0.36	1.07	4.52	1.86	2.43	1.42

	M site Occ raito[a]	Minor metal oxide content (wt%)[b]		Partition coefficient (EMPA)[c]	Partition coefficient (XRD)[d]
	Wadsleyite (M2/(M1 + M3))	Wadsleyite	Ringwoodite	$D^{Ringwoodite/Wadsleyite}$	$D^{Ringwoodite/Wadsleyite}$
SS1504 Ni	0.22	3.00	12.35	4.13	6.73

	M site Occ raito[a]		Minor metal oxide content (wt%)[b]		Partition coefficient (EMPA)[c]	Partition coefficient (XRD)[d]
	Olivine (M2/M1)	Clinoenstatite (M2/M1)	Olivine	Clinoenstatite	$D^{Oivine/Clinoenstatite}$	$D^{Oivine/Clinoenstatite}$
SS1604A Ni	0.50	0.67	1.18	0.48	2.46	1.28
SS1604B Co	0.35	1.42	1.14	0.55	2.07	1.14
SS1604C Zn	1.50	1.14	0.92	0.77	1.19	0.72

[a]Site occupancies of SS1405-1407 wadsleyite were referred to Zhang et al. (2016)

[b]Concentrations of NiO, CoO, and ZnO for SS1405-1407 wadsleyite and SS1405,1407 clinoenstatite were referred to Zhang et al. (2016)

[c]Partition coefficients (EMPA) were estimated on the basis of minor metal oxide contents

[d]Partition coefficients (XRD) were estimated on the basis of M site occupancy data listed in Table 2

positive correlation with ionic radii, implying that cation size governs the cation orderings. Considering the M1 site in enstatite is not tetragonally distorted like M1 in olivine, the CFSE is incapable of stabilizing Co^{2+} in M1, which is less distorted than M2 (Fig. 2). However, due to the increasing CFSE with decreasing metal–oxygen distances (Burns 1993), Co^{2+} is likely more stable in the slightly distorted M1 site relative to the highly distorted M2 site under the higher pressures. Consequently, for clinoenstatites synthesized at 15 GPa (SS1405-1407) (Table 2), in contrast to previous studies on enstatite (e.g., Ghose et al. 1975), Co^{2+} is more enriched in M1 relative to M2. The estimated occupancy ratios (M2/M1) of Ni^{2+}, Co^{2+}, and Zn^{2+} (Table 3) show an excellent correlation with CFSE values (Fig. 3), indicating that crystal field has more significant influences on cation ordering in a crystal in the transition zone compared to the upper mantle due to the decreasing metal–oxygen distances with rising pressure. Since the octahedral M1 sites are relatively smaller and less distorted than the M2 sites in clinoenstatite with either $C2/c$ space group or $P2_1/c$ space group (e.g., Angel et al. 1992; Morimoto et al. 1960), the cation ordering of Ni^{2+}, Co^{2+}, and Zn^{2+} in clinoenstatites are not expected to change considerably during structure transformation ($C2/c$–$P2_1/c$) on quench.

As shown in Fig. 2, the divalent metal cations in M1 and M2 in wadsleyite are each bonded to four symmetrically equivalent O4 atoms in a plane. Normal to this plane, M1 is bonded to two O3 with slightly longer bonds than the four M1–O4 bonds. For M2, however, the distances of two apical bonds (M2–O1 and M2–O2) along c axis are very different from the four M2-O4 bonds; the M2 bonded to O1 is short, whereas the bond to O2 is long, leading to a relatively distorted M2 octahedron. For M3, four metal–oxygen bonds (two M3–O1 and two M3–O3) in a plane have similar lengths, and the distances of two M3–O4 bonds normal to this plane are equivalent, resulting in a more symmetrical M3 relative to M2. Since divalent cations with a $3d^8$ high-spin configuration are expected to be stable in symmetrical octahedra (Burns 1993), Ni^{2+} prefers M1 and M3 over distorted M2 (Table 2). The defining influence of CFSE on cation orderings of Ni^{2+}, Co^{2+}, and Zn^{2+} in wadsleyite (SS1405-1407) was also observed by Zhang et al. 2016 (Fig. 3). The octahedral occupancy ratios (M2/(M1 + M3)) display a positive correlation with estimated CFSE values of Ni^{2+}, Co^{2+}, and Zn^{2+} (McClure 1957; Dunitz and Orgel 1957).

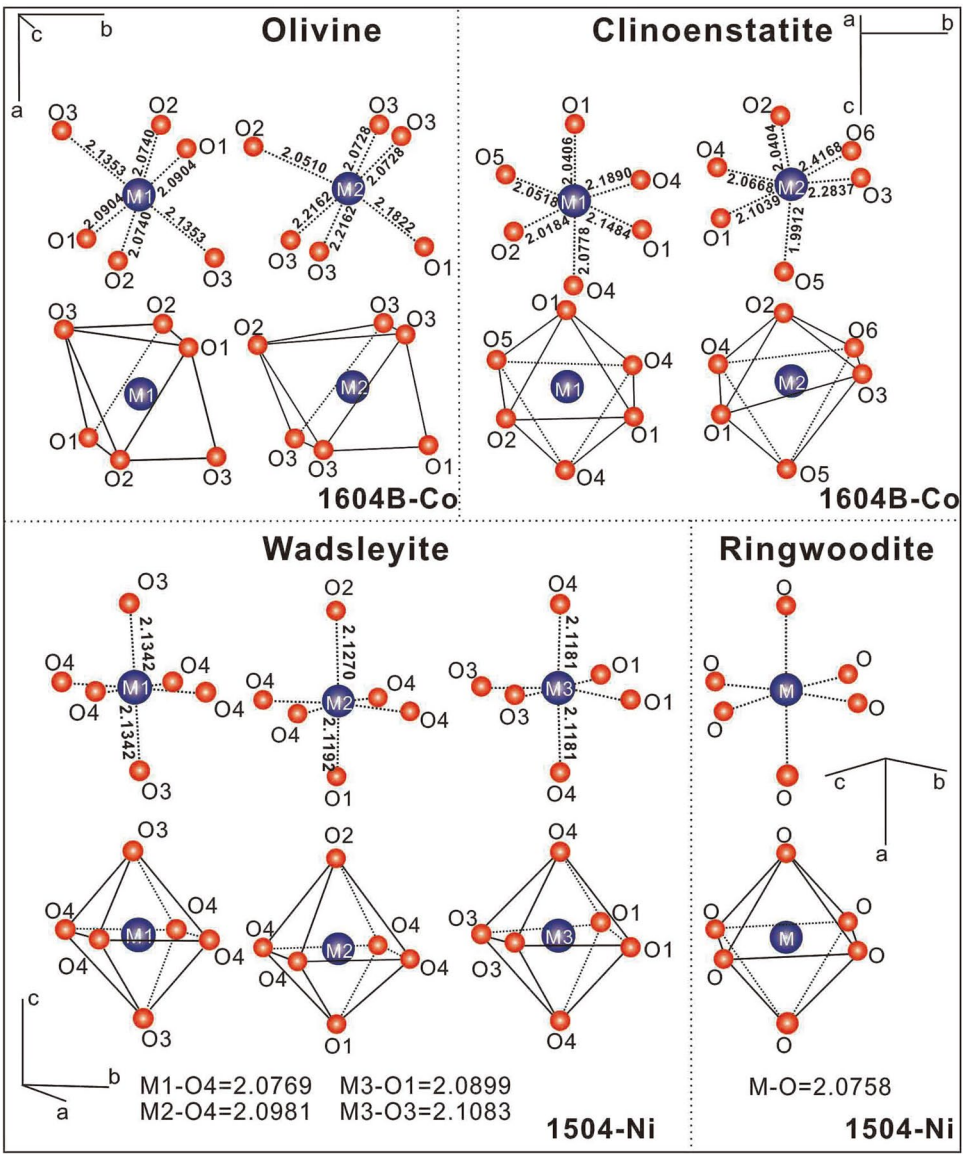

Fig. 2 Structural representations of octahedral sites in olivine, clinoenstatite, wadsleyite, and ringwoodite. Metal–oxygen distances (pm) in each site are indicated

Distributions of divalent metal ions between coexisting ferromagnesian silicates

Considering CFSE partially controls the site enrichments of ions in a crystal, it is expected to be an important influence on element distributions in coexisting silicates in the mantle. For coexisting olivine and clinoenstatite (SS1604A-C), the partition coefficients ($D^{Ol/Cen}$) of NiO, CoO, and ZnO show a strong correlation with the CFSE values of Ni^{2+}, Co^{2+}, and Zn^{2+} (Fig. 4), suggesting that divalent transition metal cations which have larger CFSE values are more likely to partition into olivine relative to coexisting clinoenstatite.

For coexisting wadsleyite and clinoenstatie (SS1405-1407), the strong correlation between partition coefficients ($D^{Wd/Cen}$) of NiO, CoO, and ZnO and the CFSE values of Ni^{2+}, Co^{2+}, and Zn^{2+} was also observed (Fig. 4). Thus, for coexisting wadsleyite and olivine, Ni^{2+}, Co^{2+}, and Zn^{2+} can be expected to partition under the influences of crystal field. Compared with olivine, wadsleyite has relatively symmetrical octahedral sites particularly for M1 and M3 (Fig. 2; e.g., Akaogi et al. 1982; Zhang et al. 2016). As a result, Ni^{2+} is more likely to substitute into wadsleyite relative to coexisting olivine due to the relatively large CFSE value and the instability of electronic configuration ($(t_{2g})^6(e_g)^2$) in distorted octahedra (Burns 1993). As shown in Fig. 4, this expectation is in accord with the reported partition coefficient ($D^{Wd/Ol}_{Ni}=2.14$; Gudfinnsson and Wood 1998) of Ni between coexisting wadsleyite and olivine. In contrast, the solubility of Ca^{2+} is relatively higher in olivine than in coexisting wadsleyite ($D^{Wd/Ol}_{Ca}=0.52$; Gudfinnsson and Wood 1998). Ca^{2+} has no CFSE, hence it is not expected to show a trend of occupying octahedra which have larger

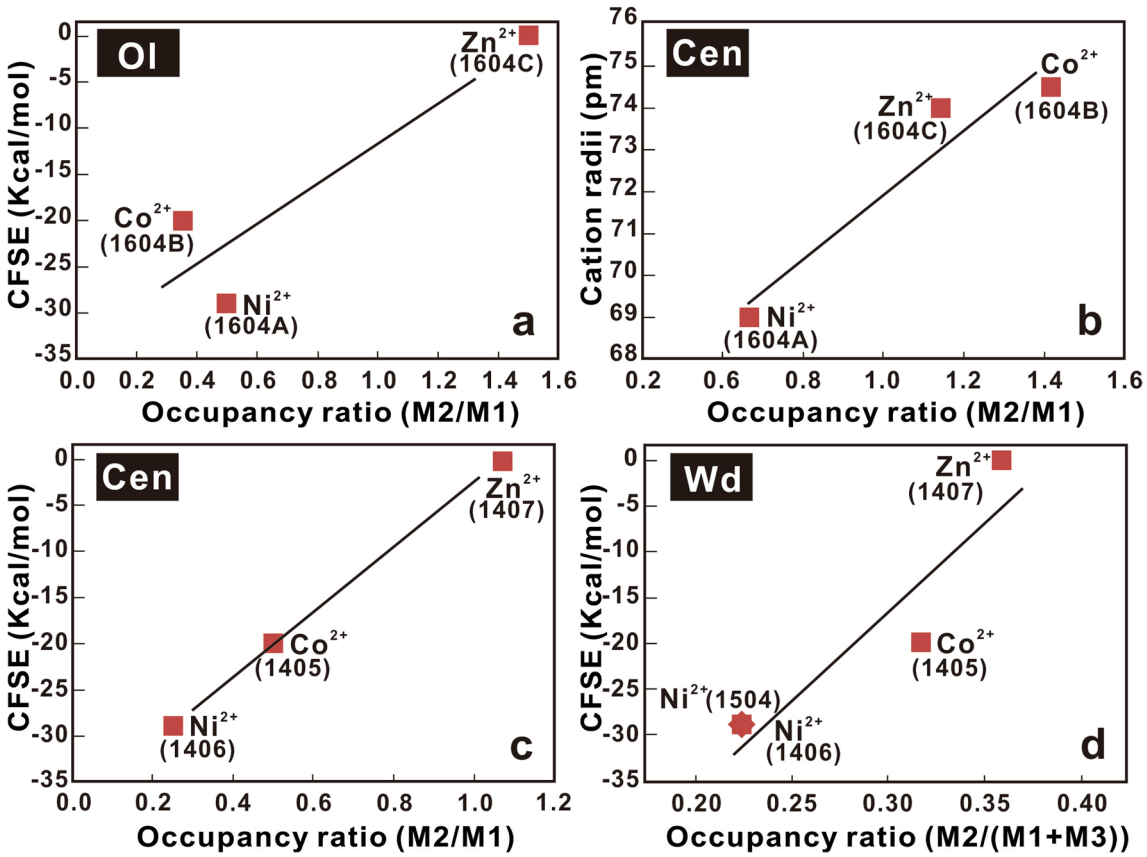

Fig. 3 **a, c, d** Correlation between occupancy ratios (M2/M1 for olivine and clinoenstatite; M2/(M1 + M3) for wadsleyite) and the crystal field stabilization energy (McClure 1957; Dunitz and Orgel 1957) for Ni^{2+}, Co^{2+}, and Zn^{2+} in olivine (SS1604A-C), clinoenstatite (SS1405-1407) and wadsleyite (SS1504 and SS1405-1407). **b** Correlation between occupancy ratios and effective ionic radii (Shannon 1976; Huheey 1983) for Ni^{2+}, Co^{2+}, and Zn^{2+} in clinoenstatite (SS1604A-C). *Ol* olivine, *Cen* clinoenstatite, *Wd* wadsleyite. Site occupancies of Ni^{2+}, Co^{2+}, and Zn^{2+} for SS1405-1407 wadsleyite were reported by Zhang et al. (2016)

CFSE. This preference can be due to the cation radius (100 pm for Ca^{2+}; Shannon 1976; Huheey 1983) and the octahedral volumes. Considering that they conducted sample syntheses in Fe-bearing system (Fo_{85}–Fo_{90}), the observed element distributions between wadsleyite and olivine in their study also indicated that the impacts of CFSE on transition metal partitioning are unlikely interfered by Fe substitution in the crystal structure. Smyth and Kawazoe (2014, unreported experiment) synthesized wadsleyites coexisting with clinopyroxenes with minor TiO_2, Cr_2O_3, V_2O_3, CoO, NiO, and ZnO (0.5–1.0 wt%, respectively) in one experiment. According to their unpublished electron microprobe analysis data, Ni, Co, and Zn preferentially partition into wadsleyite in the same order $D_{Ni}^{Wd/Cpx} > D_{Co}^{Wd/Cpx} > D_{Zn}^{Wd/Cpx}$ as mentioned above (Fig. 4), with $D_{Ni}^{Wd/Cpx} = 4.28$; $D_{Co}^{Wd/Cpx} = 3.23$; $D_{Zn}^{Wd/Cpx} = 2.65$, showing that transition metals do not strongly interact with each other on partitioning between mineral phases. Compared to wadsleyite, ringwoodite has a smaller and more symmetric octahedral site with equivalent metal-oxygen bonds (Fig. 2; Appendix Table 6). Accordingly, as shown in Tables 2 and 3, Ni^{2+} is observed to preferentially partition into ringwoodite relative to coexisting wadsleyite due to the large CFSE value and small cation size of Ni^{2+} with $D_{Ni}^{Rw/Wd} = 4.13$.

Petrological implications

Crystal field theory predicts that Ni^{2+}, because of its large CFSE value in octahedral coordination in minerals, should remain in refractory solid phases during partial fusion and are unlikely to be leached from octahedral sites in the oxide mineral structures by permeating aqueous solutions or partial melting. As a result, Ni is strongly enriched in the mantle but depleted in the continental and oceanic-crust (about 50–200 ppm) (e.g., Burns 1993). In addition, slab partial melts are also expected to have relatively low Ni concentrations (several 10 ppm at the most), since Ni is retained in residual phases in the subducting slab (e.g., Beattie et al. 1991; Straub et al. 2008). According to the

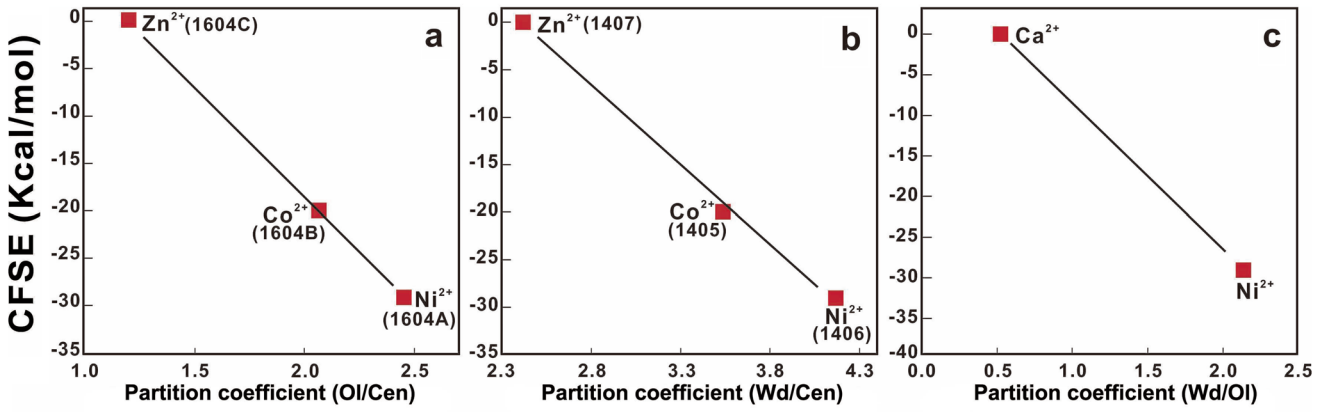

Fig. 4 **a** Correlation between partition coefficient ($D^{Ol/Cen}$) and estimated crystal field stabilization energy (McClure 1957; Dunitz and Orgel 1957) for Ni^{2+}, Co^{2+}, and Zn^{2+} in coexisting olivine and clinoenstatite (SS1604A-C). **b** Correlation between partition coefficent ($D^{Wd/Cen}$) and estimated crystal field stabilization energy (McClure 1957; Dunitz and Orgel 1957) for Ni^{2+}, Co^{2+}, and Zn^{2+} in coexisting wadsleyite (SS1405-1407 reported by Zhang et al. 2016) and clinoenstatie (SS1405-1407). **c** Correlation between partition coefficients ($D^{Wd/Ol}$) reported by (Gudfinnsson and Wood 1998) and estimated crystal field stabilization energy (McClure 1957; Dunitz and Orgel 1957) for Ni^{2+} and Ca^{2+} in coexisting olivine and wadsleyite, *Ol* olivine, *Cen* clinoenstatite, and *Wd* wadsleyite

estimated partition coefficients listed in Table 3 and previous studies on minor metal element distribution (Hakli and Wright 1967; Mercy and O'Hara 1967; Gudfinnsson and Wood 1998; Mibe et al. 2006), the distributive tendencies of Ni decrease in the order ringwoodite > wadsleyite > olivine > clinopyroxene > orthopyroxene > garnet, indicating that significant Ni-rich mineral phases in the deep upper mantle and the transition zone should be olivine, wadsleyite, and ringwoodite. Ni partitioning between the major upper-mantle phases implies that Ni-rich olivine in ultramafic rocks can be indicative of near-primary magmas.

Previous chemical analyses of the minerals in garnet-peridotite xenoliths from kimberlites showed that the partitioning of Ni between garnet and olivine is strongly temperature-dependent and the range of Ni contents in olivines is smaller than that in garnets. Therefore, Ni in garnet was proposed as a geothermometer (e.g., Griffin et al. 1989). Since crystal field effect is increasingly significant with rising pressure, Ni contents controlled by octahedral site occupancies of Ni^{2+} in garnet and coexisting olivine may also be pressure sensitive. Further constraints of the pressure effect can be achieved experimentally by crystal chemistry of Ni substitution in these mineral phases.

Conclusions

First, Ni, Co, and Zn preferentially partition into olivine and wadsleyite relative to coexisting clinoenstatite. Ni^{2+} partitions into ringwoodite relative to coexisting wadsleyite. Crystal structure refinements indicate that CFSE controls both cation ordering and transition metal partitioning in coexisting upper mantle and transition zone minerals.

Second, the cation ordering of Co^{2+} in clinoenstatite synthesized at 12 GPa is inconsistent with that in clinoenstatite synthesized at 15 GPa, implying crystal field effect on cation ordering and element distribution is more critical in the transition zone compared to the upper mantle due to decreasing metal–oxygen distances with rising pressure.

Finally, Ni partitioning between the major upper-mantle phases implies that Ni-rich olivine in ultramafic rocks can be indicative of near-primary magma.

Acknowledgements This study was supported by US National Science Foundation Grant EAR 11-13369 and EAR 14-16979 to JRS. SDJ acknowledges support from US National Science Foundation Grant EAR-1452344, the Carnegie/DOE Alliance Center, the David and Lucile Packard Foundation, and the Alexander von Humboldt Foundation. Multi-anvil experiments were supported by Bayerisches Geoinstitut Visitors Program.

References

Akaogi M, Akimoto SI, Horioka K, Takahashi KI, Horiuchi H (1982) The system $NiAl_2O_4$–Ni_2SiO_4 at high-pressures and temperatures: spinelloids with spinel-related structures. J Solid State Chem 44(2):257–267

Anderson DL (1983) Chemical-composition of the mantle. J Geophys Res 88:B41–B52

Angel RJ, Nestola F (2016) A century of mineral structures: how well do we know them? Am Miner 101(5–6):1036–1045

Angel RJ, Chopelas A, Ross NL (1992) Stability of high-density clinoenstatite at upper-mantle pressures. Nature 358(6384):322–324

Annersten H, Ericsson T, Filippidis A (1982) Cation ordering in Ni–Fe olivines. Am Miner 67(11 – 1):1212–1217
Bancroft GM, Burns RG (1967) Interpretation of electronic spectra of iron in pyroxenes. Am Miner 52(9–10):1278–1287
Beattie P, Ford C, Russell D (1991) Partition-coefficients for olivine-melt and ortho-pyroxene-melt systems. Contrib Miner Petr 109(2):212–224
Birle JD, Gibbs GV, Moore PB, Smith JV (1968) Crystal structures of natural olivines. Am Miner 53(5–6):807–824
Burns RG (1993) Mineralogical applications of crystal field theory. Cambridge University Press, Cambridge
Cromer DT, Mann JB (1968) X-ray scattering factors computed from numerical Hartree-Fock wave functions. Acta Crystall A Crys A 24:321–325
de Waal SA (1978) The nickel deposit at Bon Accord, Barberton, South Africa-a proposed paleometeorite. In: Verwoerd WJ (ed) Mineralisation in metamorphic terranes. Geological Society of South Africa, Johannesburg
Demouchy S, Deloule E, Frost DJ, Keppler H (2005) Pressure and temperature-dependence of water solubility in Fe-free wadsleyite. Am Miner 90(7):1084–1091
Dobrzhinetskaya L, Green HW, Wang S (1996) Alpe Arami: a peridotite massif from depths of more than 300 kilometers. Science 271(5257):1841–1845
Dunitz JD, Orgel LE (1957) Electronic properties of transition-metal oxides. II. Cation distribution amongst octahedral and tetrahedral sites. J Phys Chem Solids 3(3–4):318–323
Finger LW, Hazen RM, Zhang JM, Ko JD, Navrotsky A (1993) The effect of Fe on the crystal structure of wadsleyite β-$(Mg_{1-x}Fe_x)SiO_4$, $0.00 \leq x \leq 0.40$. Phys Chem Miner 19(6):361–368
Ghose S, Wan C, Okamura P, Ohashi H, Weidner JR (1975) Site preference and crystal-chemistry of transition-metal ions in pyroxenes and olivines. Acta Crystallogr A 31:S76–S76
Green HW, Dobrzhinetskaya L, Riggs EM, Jin ZM (1997) Alpe Arami: a peridotite massif from the mantle transition zone? Tectonophysics 279(1–4):1–21
Griffin WL, Cousens DR, Ryan CG, Sie SH, Suter GF (1989) Ni in chrome pyrope garnets: a new geothermometer. Contrib Miner Petrol 103:199–202
Gudfinnsson GH, Wood BJ (1998) The effect of trace elements on the olivine-wadsleyite transformation. Am Miner 83(9–10):1037–1044
Hacker BR, Sharp T, Zhang RY, Liou JG, Hervig RL (1997) Determining the origin of ultrahigh-pressure lherzolites. Science 278(5338):702–704
Hakli TA, Wright TL (1967) Fractionation of nickel between olivine and augite as a geothermometer. Geochim Cosmochim Acta 31(5):877–884
Harris PG, Reay A, White IG (1967) Chemical composition of upper mantle. J Geophys Res 72(24):6359–6369
Hofmann AW (1988) Chemical differentiation of the Earth: the relationship between mantle, continental-crust, and oceanic-crust. Earth Planet Sc Lett 90(3):297–314
Huheey JE (1983) Inorganic chemistry: principles of structure and reactivity, 3rd edn. Harper & Row, New York
Liu L-G, Bassett WA (1986) Elements, oxides and silicates. High-pressure phases with implications for the Earth's interior. Oxford University Press, Oxford
McCarty RJ, Palke AC, Stebbins JF, Hartman JS (2015) Transition metal cation site preferences in forsterite (Mg_2SiO_4) determined from paramagnetically shifted NMR resonances. Am Miner 100(5–6):1265–1276
McClure DS (1957) The distribution of transition metal cations in spinels. J Phys Chem Solids 3(3–4):311–317
McDonough WF, Sun SS (1995) The composition of the Earth. Chem Geol 120(3–4):223–253
Mercy E, Ohara MJ (1967) Distribution of Mn Cr Ti and Ni in coexisting minerals of ultramafic rocks. Geochim Cosmochim Acta 31(12):2331–2341
Mibe K, Orihashi Y, Nakai S, Fujii T (2006) Element partitioning between transition-zone minerals and ultramafic melt under hydrous conditions. Geophys Res Lett 33:16
Morimoto N, Appleman DE, Evans HT (1960) The crystal structures of clinoenstatite and pigeonite. Z Kristallogr 114:120–147
Nestola F, Tribaudino M, Ballaran DB (2004) High pressure behavior, transformation and crystal structure of synthetic iron-free pigeonite. Am Miner 89(1):189–196
Ringwood AE (1958) The constitution of the mantle-II: further data on the olivine-spinel transition. Geochim Cosmochim Acta 13(4):303–321
Ringwood AE (1967) Pyroxene-garnet transformation in Earth's mantle. Earth Planet Sci Lett 2(3):255–263
Shannon RD (1976) Revised effective ionic-radii and systematic studies of interatomic distances in halides and chalcogenides. Acta Crystallogr A 32(Sep1):751–767
Sheldrick GM (1997) SHELXS97 and SHELXL97. Program for crystal structure solution and refinement. University of Göttingen, Göttingen
Smith EM, Shirey SB, Nestola F, Bullock ES, Wang JH, Richardson SH, Wang WY (2016) Large gem diamonds from metallic liquid in Earth's deep mantle. Science 354(6318):1403–1405
Smyth JR (1969) Orthopyroxene-high-low clinopyroxene inversions. Earth Planet Sci Lett 6(5):395–405
Smyth JR, Holl CM, Frost DJ, Jacobsen SD (2004) High pressure crystal chemistry of hydrous ringwoodite and water in the Earth's interior. Phys Earth Planet Interior 143:271–278
Smyth JR, Bolfan-Casanova N, Avignant D, El-Ghozzi M, Hirner SM (2014) Tetrahedral ferric iron in oxidized hydrous wadsleyite. Am Miner 99(2–3):458–466
Stachel T, Harris JW (2008) The origin of cratonic diamonds—constraints from mineral inclusions. Ore Geol Rev 34(1–2):5–32
Straub SM, LaGatta AB, Pozzo ALMD., Langmuir CH (2008) Evidence from high-Ni olivines for a hybridized peridotite/pyroxenite source for orogenic andesites from the central Mexican Volcanic Belt. Geochem Geophy Geosyst 9:3
Tokonami M (1965) Atomic scattering factor for O^{2-}. Acta Crystallogr 19:486–486
Ye Y, Schwering RA, Smyth JR (2009) Effects of hydration on thermal expansion of forsterite, wadsleyite, and ringwoodite at ambient pressure. Am Miner 94(7):899–904
Zhang L, Smyth JR, Allaz J, Kawazoe T, Jacobsen SD, Jin ZM (2016) Transition metals in the transition zone: crystal chemistry of minor element substitution in wadsleyite. Am Miner 101(9–10):2322–2330